Dominant Reaction Pathways by Quantum Computing

Philipp Hauke,[1] Giovanni Mattiotti,[2] and Pietro Faccioli[2, 3]

[1]*INO-CNR BEC Center and Department of Physics,*
University of Trento, Via Sommarive 14, I-38123 Trento, Italy
[2]*Department of Physics, University of Trento, Via Sommarive 14, I-38123 Trento, Italy*
[3]*INFN-TIFPA, Via Sommarive 14, I-38123 Trento, Italy*

(Dated: July 29, 2020)

Characterizing thermally activated transitions in high-dimensional rugged energy surfaces is a very challenging task for classical computers. Here, we develop a quantum annealing scheme to solve this problem. First, the task of finding the most probable transition paths in configuration space is reduced to a shortest-path problem defined on a suitable weighted graph. Next, this optimization problem is mapped into finding the ground state of a generalized Ising model, a task that can be efficiently solved by a quantum annealing machine. This approach leverages on the quantized nature of qubits to describe transitions between different system's configurations. Since it does not involve any lattice space discretization, it paves the way towards biophysical applications of quantum computing based on realistic all-atom models.

Introduction. Thermally activated processes, and in particular conformational transitions of macromolecules, play a key role in many research fields at the interface between physics, chemistry, biology. Molecular Dynamics (MD) offers a theoretically sound framework to investigate these processes by sampling the corresponding transition path ensembles at the atomic level of resolution. Unfortunately, MD is very computationally inefficient whenever the system's energy landscape is rugged.

To overcome the limitations of MD, much effort has been put over the last two decades toward devising enhanced sampling algorithms [1]. In particular, an exponential speed-up of the computational efficiency can be obtained by introducing specific biasing forces which promote the escape rate from metastable minima [2–4]. All these methods typically require prior knowledge about the reaction coordinate or the system's slowest Collective Variables (CVs). Unfortunately, the identification of these variables is in general a very challenging task, and a sub-optimal choice can hamper the convergence or introduce systematic errors.

During the last several years, quantum computing machines have grown exponentially both in size and performance, to a point that it is now realistic to foresee the onset of quantum supremacy in key computational problems [5]. It is therefore both important and timely to address the question whether quantum computation can be employed to identify statistically relevant transition pathways in high-dimensional rugged energy surfaces, without having to rely on any choice of CVs.

In recent years, progress has been made on designing quantum annealing algorithms for chemistry and biology applications [6–11]. Yet, only a few applications of quantum computation to classical molecular sampling problems have been reported to date [12, 13]. Arguably, the key issue that is limiting the application of quantum computers to molecular mechanics is the fact that quantum machines are best suited to tackle *discrete* problems. For this reason, to the best of our knowledge, all the quantum computing algorithms for sampling and energy optimization of classical molecular structures rely on simplified lattice models. While these models have provided valuable insight into the general statistical mechanical properties of biopolymers [14], the lack of structural and chemical detail hampers their applicability to investigate realistic biophysical systems.

In this work, we develop a rigorous approach to finding the most statistically relevant transition paths in a thermally activated reaction using a quantum computing machine. Our method does not require lattice discretization. Thus, it is in principle applicable to realistic molecular models, e.g. based on all-atom force fields.

The basic idea is to first use molecular simulations based on classical computing to generate large data sets of conformations, mostly concentrated in the transition region between the given reactant and product states. The key point here is that this set of molecular configurations is not required to sample any physically meaningful distribution, therefore it can be generated in a computationally very efficient way, possibly relying on massively distributed schemes. For example, one could merge into a single data set configurations obtained using different algorithms, such as machine-learning schemes for uncharted manifold learning [15] and plain MD performed at very high temperature.

The next step is to assign *a posteriori* a relative statistical weight to all the reactive trajectories that can be drawn by connecting the configurations in this sparse dataset. Indeed, using the so-called Dominant Reaction Pathways (DRP) formalism [16] the most probable transition pathways connecting given initial and final configurations can be rigorously obtained from a least-action principle. After restricting the molecular configuration space to the previously generated ensemble of molecular structures, the DRP variational problem becomes equivalent to a shortest path problem formulated on a discrete weighted graph, which can be tackled by quantum annealing. The key difference to other proposed quantum computing approaches for molecular sampling [12, 13] is that the discretization required to run on a quantum
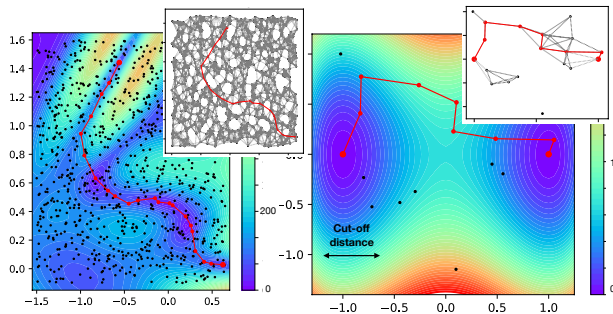
Figure 1. Minimum energy path calculated in the Müller Brown energy surface using the Dijkstra algorithm (left panel) and in the double-well potential by simulated annealing of the Ising Hamiltonian (right panel). In both panels, the heat-map displays the potential energy in units of $k_B T$, the points have been sampled from a flat distribution, and the insets show the associated weighted graphs.

computing machine is performed at the level of the system's configuration space and that the points in this configuration space are defined in continuum space and are generated using a classical computer.

Dominant Reaction Pathways. Let us begin by briefly reviewing the DRP formalism. The starting assumption is that the system's structural dynamics can be modeled by a set of over-damped Langevin equations:

$$\dot{\mathbf{q}}_i = -\frac{D}{k_B T} \nabla_i U(\mathbf{q}) + \eta_i(t), \qquad i = 1, \ldots N. \quad (1)$$

$\mathbf{q}_i$ denotes the position of the $i-$th particle in the system, and D is the diffusion coefficient (here chosen for simplicity to be the same for all particles). $U(Q)$ is the molecular potential energy and $Q = (\mathbf{q}_1, \ldots \mathbf{q}_N)$ is the $3N-$dimensional coordinate in the system's configuration space, while $\eta_i(t)$ is a delta-correlated white noise obeying the fluctuation-dissipation relationship $\langle \eta_i(t)\eta_i(0) \rangle = 2D\delta_{ij}\delta(t)$. The over-damped limit is appropriate to describe the dynamics of proteins, with a time-resolution on the order of picoseconds or lower.

The probability of finding the system in a conformation Q_f at time t, conditioned to be at the conformation Q_0 at the initial time t_0 can be expressed as a path integral,

$$P(Q_f, t|Q_0, t_0) = e^{-\frac{(U(Q_f)-U(Q_i))}{2k_B T}} \int_{Q_0}^{Q_f} \mathcal{D}Q \, e^{-S_{\text{eff}}[Q]} \quad (2)$$

where $S_{\text{eff}}[Q]$ is called the effective action and reads

$$S_{\text{eff}}[Q] = \int_{t_0}^{t} d\tau \left(\frac{\dot{Q}^2}{4D} + V_{\text{eff}}[Q(\tau)] \right), \quad (3)$$

while $V_{\text{eff}}(Q) = \frac{D}{4(k_B T)^2} \left((\nabla U(Q))^2 - 2k_B T \nabla^2 U(Q) \right)$.

The DRP approach focuses on the most probable reactive trajectories and is based on the saddle-point approximation of the functional integral (2). The functional minima of the effective action $S_{\text{eff}}[Q]$, are called dominant paths and obey the Newton-type equations of motion $2D\ddot{\mathbf{q}}_i = \nabla_i V_{\text{eff}}(Q)$. This implies the conservation of

the so-called effective energy $E_{\text{eff}} = \frac{\dot{Q}^2}{4D} - V_{\text{eff}}(Q)$ along the dominant paths. Using this property, it is possible to show that the saddle-points of the functional integral (2) coincide with the minima of the Hamilton–Jacobi (HJ) functional [16, 18]

$$S_{\text{HJ}}[Q] = \int_{Q_0}^{Q_f} dl \sqrt{\frac{1}{D}(V_{\text{eff}}[Q(l)] + E_{\text{eff}})}, \quad (4)$$

where $dl = \sqrt{dQ^2}$ is an infinitesimal conformational displacement along the dominant path. The effective energy parameter E_{eff} implicitly sets the time interval $t - t_0$ entering Eq. (2), through the equation $t - t_0 = \int_{Q_0}^{Q_f} dl \{4D(V_{\text{eff}}[Q(l)] + E_{\text{eff}})\}^{-1/2}$. For this time-scale to be on the order of the typical transition path time, the effective energy must be chosen $E_{\text{eff}} \sim -V_{\text{eff}}(Q_i)$ [17, 19].

In molecular simulations, the HJ formulation of the saddle-point condition leads to a dramatic computational advantage with respect to the standard (i.e. time-dependent) formulation. This is because the typical root-mean-square distance between kinetically distant molecular configurations can be at most two orders of magnitude larger than the atomic size. As a consequence, only a few tens of configurations are usually sufficient for an accurate representation of the line integral in the HJ functional (4). In contrast, to accurately discretize the time integral in the effective action (3) one would need to use time steps dt on the order of fs, while the typical transition path times for complex macromolecular transitions (such as e.g. protein folding) are about 9 orders of magnitude larger. We emphasize again this point, since it is a cornerstone of our approach: using the HJ formalism it is possible to assign correct statistical weight to the paths that are obtained connecting configurations in the previously generated sparse dataset, even though the typical time it would take the system to diffuse from one of these configurations to a nearest neighbor may be as long as several ns.

Shortest-path problem formulation. The HJ variational condition can be rigorously mapped into a shortest-path problem on a discrete graph. To this end, we assign a vertex in the graph (labelled $i, j = 1 \ldots |\mathcal{V}|$) to each molecular configuration in the previously generated dataset and identify the initial conformation Q_0 with the source s and the final conformation Q_f with the target t. Next, we define a set $\mathcal{E}$ of directed edges (ij) that connect vertices i and j. Each directed edge is assigned a weight (or 'cost')

$$w_{(ij)} = \frac{\Delta l_{(ij)}}{2\sqrt{D}} (L_i + L_j)$$

$$(5)$$

with $L_i = \sqrt{V_{\text{eff}}(Q_i) + E_{\text{eff}}}$ and $\Delta l_{(ij)} = \sqrt{(Q_i - Q_j)^2}$. In this notation, the target function to minimize on the network is $S_{\text{HJ}} = \sum_{k=1}^{M} w_{(i_k i_{k+1})}$, with $i_1 = $ s and $i_M = $ t. To ensure that the HJ functional is correctly represented by discrete paths on the network, we take only edges into account with a cost below a given cutoff W_c. We note

that this condition can drastically reduce the complexity of our optimization problem, as for a judicious choice of W_c the number of edges will become proportional to the number of vertices $|\mathcal{V}|$ rather than $|\mathcal{V}|^2$.

To summarize, so far we have mapped the problem of finding the dominant transition pathways in a high-dimensional continuous energy landscape into a shortest path problem in the weighted graph $(\mathcal{V}, \mathcal{E})$. It is important to emphasize that, in its original continuous-space formulation, the DRP least-action principle corresponds to an NP-hard global optimization problem [16, 18]. This computational limitation hampered the straightforward application of this approach to investigate large macromolecular transitions. However, after mapping the DRP least-action principle into a shortest path problem on the graph, it is possible to rely on very efficient discrete optimization algorithms such as the Dijkstra algorithm [24].

It is convenient to illustrate how this path finding algorithm works in a prototypical toy model for rare activated transition. Namely, we consider the diffusion of a point-particle in the Müller-Brown two-dimensional energy surface, displayed in Fig. 1 —the functional form used is reported in the Appendix—. Our goal is to find the dominant reaction path connecting the local energy minimum $Q_R = -(0.56, 1.44)$ to the energy minimum at $Q_P = (0.62, 0.03)$. To facilitate the visual assessment of the results, we focus on the low-temperature regime, in which the SH functional reduces to $S_{\mathrm{HJ}} = (k_B T/2)^{-1} \int_{Q_i}^{Q_f} dl |\nabla U[Q(l)]|$. Thus, in this limit, the dominant pathway reduces to the minimum-energy path [18]. As a first step, we generated an ensemble of 2000 configurations by randomly sampling points in the region $q_1 \in [-1.5, 0.65], q_2 \in [0.65, 1.6]$. In applications to macromolecular systems, this random ensemble of points would be replaced by molecular conformations generated on a classical machine. We emphasize that the flat distribution of points on the plain does not correspond to any physically meaningful ensemble. Next, we built the sparse network connecting each point to its 10 nearest neighbors and assigned a weight to each edge proportional to the corresponding contribution $w_{(ij)}$ to the HJ action (inset in the left panel of Fig. 1). Finally, to compute the shortest path on this graph we resorted to the Dijkstra algorithm. The result is the red line, which clearly provides a very accurate representation of the minimum-energy path in this landscape.

Finding the Shortest-Path by Quantum Computing. Let us now tackle the problem of formulating the shortest path problem in a way amenable to global optimization through a quantum annealing machine. To this end, we consider the linear programming formulation of the shortest path problem: We introduce the binary variables $x_{(ij)} = 0, 1$, located at edges (ij). $x_{(ij)} = 1$ means the edge (ij) is part of the shortest path, while $x_{(ij)} = 0$ means it is not. We emphasize that in our directed graph, we distinguish between (ij) and (ji). The task of finding the shortest path is then translated into minimizing the target function $\sum_{(ij)\in\mathcal{E}} w_{(ij)} x_{(ij)}$ subject to the constraints

$$\forall i : \sum_{j\in\mathcal{V}} x_{(ij)} - \sum_{j\in\mathcal{V}} x_{(ji)} = \begin{cases} 1, & \text{if } i = \mathrm{s}; \\ -1, & \text{if } i = \mathrm{t}; \\ 0, & \text{otherwise.} \end{cases} \quad (6)$$

These constraints represent a conservation of flux: since we are searching for a connected path, at each vertex the number of incoming edges must equal the number of outgoing edges. Exceptions are s, where the number of outgoing edges is larger by one than the number of incoming edges, and t, where the converse is true.

These can be cast into the form of a quadratic function

$$H_A = A \left\{ \left[\sum_{j\in\mathcal{V}} \left(x_{(\mathrm{s}j)} - x_{(j\mathrm{s})} \right) - 1 \right]^2 + \right.$$

$$\left. \left[\sum_{j\in\mathcal{V}} \left(x_{(\mathrm{t}j)} - x_{(j\mathrm{t})} \right) + 1 \right]^2 + \sum_{\substack{i\in\mathcal{V} \\ i\neq\mathrm{s},\mathrm{t}}} \left[\sum_{j\in\mathcal{V}} \left(x_{(ij)} - x_{(ji)} \right) \right]^2 \right\}$$

$$(7)$$

Note that in the above terms, the summation over j is restricted to the vertices connected to s, t, and i, respectively. Defining in addition the cost function to the HJ functional

$$H_B = B \sum_{(ij)\in\mathcal{E}} w_{(ij)} x_{(ij)}, \quad (8)$$

the shortest path problem can be reformulated as: Find the set of binary variables $x_{(ij)}$ that minimize the classical cost function $H = H_A + H_B$. Note that, in order for H_A to be a hard constraint, we require the ratio between coupling constants A/B to be sufficiently large. A rigorous condition is $A/B > |\mathcal{E}| W_c$, where $|\mathcal{E}|$ is the number of edges, but in practice smaller values often suffice.

In order to solve the problem with a quantum processing device, we re-interpret the classical cost function H as a quantum mechanical Hamiltonian described by z-Pauli-components of spins 1/2, defined by $\sigma^z_{(ij)} = 2x_{(ij)} - 1$. These spins 1/2 are to be encoded in the qubits of the quantum annealer. The resulting generalized Ising Hamiltonian is explicitly reported in the Appendix.

In quantum annealing, the problem of finding the minimum energy configuration of H is solved in the following way [20–22]. The qubits are initialized in the ground state of an easily solvable Hamiltonian that does not commute with H, say $H_{\mathrm{in}} = -h \sum_{(ij)} \sigma^x_{(ij)}$. Then, the qubit system is subjected to a time-dependent Hamiltonian $a(t)H_{\mathrm{in}} + b(t)H$, with scheduling functions $a(t)$ and $b(t)$. These are chosen such that initially $a(0) = 1$ and $b(0) = 0$, while at the end of the protocol at t_{sweep} one has $a(t_{\mathrm{sweep}}) = 0$ and $b(t_{\mathrm{sweep}}) = 1$. In this way, the Hamiltonian is transformed from the simple H_{in} to the complex problem Hamiltonian H. If the sweep is performed sufficiently slowly, by the adiabatic theorem

the system remains in its instantaneous ground state all the way through the sweep. That is, the final state at the end of the protocol is the ground-state of H, i.e. the solution to the shortest-path problem. Note that in current practical devices there is considerable coupling to the environment, such that the sweep is not fully coherent and higher levels can be populated. This deteriorates the success probability and makes it difficult to derive rigorous proofs about any quantum advantage. Despite these limitations, quantum annealing has been used successfully for a large number of problems, including many NP-complete as well as applications ranging from search-engine ranking over machine learning to quantum chemistry, and various ways forward to improve the performance of quantum annealing devices have been identified; see Refs. [20–22] for recent reviews.

In principle, since our problem requires only an undirected solution of the shortest path, one could e.g. adapt the algorithm developed in Ref. [23]. There, the qubits encode the vertices rather than the links. The final state of the quantum computer then returns the vertices that lie on the optimal path, but not their order, which thus requires additional postprocessing. If there is a unique shortest path, the number of qubits required for the algorithm of Ref. [23] scales as $|\mathcal{V}|$. In the presence of several shortest paths, the number of links in the shortest path Δ needs to be known and the scaling grows to $|\mathcal{V}|\Delta$. In contrast, the qubit requirement of our algorithm scales slower than $2|\mathcal{V}|c$, where c denotes the number of edges at the site with the largest connectivity, and no *a priory* knowledge of properties of the shortest path is necessary.

Let us now illustrate how the dominant path is obtained from the ground-state of our generalized Ising Hamiltonian. While we have designed this algorithm to be implemented on a quantum annealing machine, here we have resorted to classical simulated annealing. It should be kept in mind that a spin-glass formulation of the shortest path problem is inefficient when implemented on a classical computer. To keep the computational effort tractable, we chose to consider a smooth two-dimensional double well potential (shown in the right panel of Fig. 1 and defined in Appendix), for which only 20 random configurations on the plane were sufficient to achieve a coarse-grained representation of configuration space. We implemented the Ising system associated to a graph in which the nearest neighbors of each configuration were selected according to cut-off distance of 0.6, leading to 78 spins. The right panel of Fig.1 shows the minimum energy path obtained after 80000 steps of simulated annealing of the Ising Hamiltonian with $A = 100$ and $B = 50$, with an inverse thermal energy ranging from $\beta = 5 \times 10^{-3}$ to $\beta = 6 \times 10^{-2}$. This result provides the optimal approximation of the minimum energy path, given the very coarse-grained discrete representation of configuration space and the cut-off distance.

How many qubits are expected to be necessary for a realistic application to a macromolecular transition? As reference for the minimal number of conformations re-

quired to represent the transition region of a complex reaction, we take the number of micro-states used in Markov State stochastic models to represent the folding process of very small globular proteins, which is of the order 10^4 [25]. Assuming an average connectivity of ~ 10 edges per vertex we arrive at a minimal number of qubits on the order of 10^5.

To date, the largest quantum annealing machines have $o(10^3)$ qubits and are not yet in a position to outperform classical computers in shortest path calculation. However, if the current exponential growth in quantum processors continues, the proposed method has the potential to play a game changing role in the field of molecular simulations, enabling the investigation of increasingly complex and rare transitions.

Our approach represents a new paradigm for tackling biophysical problems using quantum optimization: Instead of discretizing real space onto a lattice —which would hamper the application to realistic systems of biological interest— it makes efficient use of the quantized nature of the qubit register to represent a discrete set of system's configurations, each of which can be arbitrarily complex. In addition, it can capitalize on recently developed powerful machine learning techniques to perform an uncharted exploration of complex energy landscapes.

Appendix A: Energy Surfaces

The potential energy of the Müller-Brown energy surface [26] used in the illustrative example in the main text is

$$U(x,y) = \sum_{i=1}^{4} A_i e^{a_i(x-x_0^i)^2 + b_i(x-x_0^i)(y-y_0^i) + c_i(y-y_0^i)^2} \quad (A1)$$

where the parameters are reported in the Table.

Table I. Parameters of the Müller-Brown potential

A_1=-200,	A_2=-100,	A_3=-170,	A_4=15
x_0^1=1,	x_0^2=0,	x_0^3=-0.5,	x_0^4=1
y_0^1=0,	y_0^2=0.5,	y_0^3=-1.5,	y_0^4=1
a_1=1,	a_2=-1,	a_3=-6.5,	a_4=0.7
b_1=0,	b_2=0,	b_3=-11,	b_4=0.6,
c_1=-10,	c_2=-10,	c_3=-6.5,	c_4=0.7.

The energy surface of the two-dimensional double-well is given by

$$U(x,y) = u_0(x^2 - x_0^2)^2 + \frac{1}{2}k_0 y^2 \quad (A2)$$

We set $u_0 = k_B T = 1$, and $k_0 = 2$ and $x_0 = 1$ in appropriate units.

Appendix B: Generalized Ising Hamiltonian

result is

$$H_A = H_{(\mathrm{s})} + H_{(\mathrm{t})} + H_{(ij)} \tag{B1}$$

$$
H_{(\mathrm{s})} = \frac{A}{4}\left\{ 4 + \sum_{i,j\in\mathcal{V}} (\sigma^z_{(\mathrm{s}j)}\sigma^z_{(\mathrm{s}i)} + \sigma^z_{(j\mathrm{s})}\sigma^z_{(i\mathrm{s})} - \sigma^z_{(j\mathrm{s})}\sigma^z_{(\mathrm{s}i)} \right.
$$
$$
\left. - \sigma^z_{(\mathrm{s}j)}\sigma^z_{(i\mathrm{s})}) - 4\sum_{i\in\mathcal{V}}\sigma^z_{(\mathrm{s}i)} + 4\sum_{i\in\mathcal{V}}\sigma^z_{(i\mathrm{s})} \right\} \tag{B2}
$$

$$
H_{(\mathrm{t})} = \frac{A}{4}\left\{ 4 + \sum_{i,j\in\mathcal{V}} (\sigma^z_{(\mathrm{t}j)}\sigma^z_{(\mathrm{t}i)} + \sigma^z_{(j\mathrm{t})}\sigma^z_{(i\mathrm{t})} - \sigma^z_{(j\mathrm{t})}\sigma^z_{(\mathrm{t}i)} \right.
$$
$$
\left. - \sigma^z_{(\mathrm{t}j)}\sigma^z_{(i\mathrm{t})}) + 4\sum_{i\in\mathcal{V}}\sigma^z_{(\mathrm{t}i)} - 4\sum_{i\in\mathcal{V}}\sigma^z_{(i\mathrm{t})} \right\} \tag{B3}
$$

$$
H_{(ij)} = \frac{A}{4}\left\{ \sum_{\substack{i,j,k\in\mathcal{V}\\ i\neq \mathrm{s},\mathrm{t}}} (\sigma^z_{(ij)}\sigma^z_{(ik)} + \sigma^z_{(ji)}\sigma^z_{(ki)} - \sigma^z_{(ji)}\sigma^z_{(ik)} \right.
$$
$$
\left. - \sigma^z_{(ij)}\sigma^z_{(ki)}) \right\} \tag{B4}
$$

while, dropping an irrelevant constant in H_B, we get

$$H_B = \frac{B}{2}\sum_{(ij)\in\mathcal{E}} w_{(ij)}\sigma^z_{(ij)}. \tag{B5}$$

The task is now to find the ground state of the qubit (Ising-spin) Hamiltonian $H = H_A + H_B$.

In practice, the shortest path will avoid loops, and the constraints in Eq. (6) of the main text then amount to

$$
\forall i: \left(\sum_{j\in\mathcal{V}} x_{(ij)}, \sum_{j\in\mathcal{V}} x_{(ji)}\right) = \begin{cases} (1,0), & \text{if } i = \mathrm{s}; \\ (0,1), & \text{if } i = \mathrm{t}; \\ (0,0) \text{ or } (1,1), & \text{else.} \end{cases} \tag{B6}
$$

One may implement this observation with an additional set of quadratic terms such as $\sum_{\substack{i\in\mathcal{V}\\ i\neq\mathrm{s},\mathrm{t}}} (\sum_{j\in\mathcal{V}} x_{(ij)} - 1)^2$ etc., which one can add to Eq. (B1). In addition, the edges leading into s and out of t can be eliminated. We find the more flexible formulation in Eq. (6) of the main text that allows for loops to be sufficient for our purposes.

The generalized Ising Spin formulation of the shortest-path problem on the discrete graph is straightforwardly obtained from the quadratic function (7) of the main text by means of the substitution $x_{(ij)} = (\sigma^z_{(ij)} + 1)/2$. The

---

[1] Y.I. Yang, Q. Shao, J. Zhang, L. Yang, and Y.Q. Gao, J. Chem Phys. **151** 070902 (2019)

[2] A. Laio, M. Parrinello, Proc. Natl. Acad. Sci. USA **99** 12562 (2002).

[3] M. A. Cuendet and M. E. Tuckerman, J. Chem. Theory Comput. **10**, 2975 (2014).

[4] S. a Beccara, L. Fant, and P. Faccioli, Phys. Rev. Lett. **114**, 098103 (2015).

[5] F. Arute et al., Nature **574**, 505–510 (2019).

[6] M. Streif, F. Neukart, M. Leib, In: Feld S., Linnhoff-Popien C. (eds) Quantum Technology and Optimization Problems. QTOP 2019. Lecture Notes in Computer Science, vol 11413. Springer, Cham (2018).

[7] R.Y. Li, R.D. Felice, R. Rohs, D.A. Lidar, npj Quantum Information **4**, 14 (2018).

[8] S.N. Genin, I.G. Ryabinkin, A.F. Izmaylov, arXiv:1901.04715 (2019).

[9] Y. Cao et al., Chem. Rev. **119**, 1085610915 (2019).

[10] S. Matsuura, T. Yamazaki, L. Huntington, A. Zaribafiyan, New J. Phys. **22**, 053023 (2020).

[11] C. Outeiral, M. Strahm, J. Shi, G.M. Morris, S.C. Benjamin, C.M. Deane, WIREs Comput. Mol. Sci. e1481

(2020).

[12] A. Perdomo-Ortiz, N. Dickson, M. Drew-Brook, G. Rose, and A. Aspuru-Guzik, Scientific Reports **2**, 571 (2012).

[13] L.H. Lu and Y.Q. Li Chin. Chem. Lett. **36**, 080305 (2019).

[14] L. Mirny and E. Shakhnovich Ann. Rev. Biophys. Biomol. Struct. **30** 361 (2001).

[15] E. Chiavazzo, R. Covino, R., Coifman, C. W. Gear, A. S. Georgiou, G. Hummer, and I. G. Kevrekidis, Proc. Nat. Acad. Sci. U.S.A. **114** (28), E5494 (2017).

[16] P. Faccioli, M. Sega, F. Pederiva, and H. Orland, Phys. Rev. Lett. **97**, 108101 (2006).

[17] M. Sega,P. Faccioli, F. Pederiva,G. Garberoglio, and H. Orland, Phys. Rev. Lett. **99**, 118102 (2007).

[18] R. Elber and D. Shalloway, J. Chem. Phys. **112**, 5539 (2000).

[19] P. Faccioli and F. Pederiva Phys. Rev. **E 86**, 061916 (2012)

[20] T. Albash, D.A. Lidar, Rev. Mod. Phys. **90**, 015002 (2018).

[21] S.E. Venegas-Andraca, W. Cruz-Santos, C. McGeoch, M. Lanzagorta, Contemporary Physics **59**, 174197 (2018).

[22] P. Hauke, H.G. Katzgraber, W. Lechner, H. Nishimori, W.D. Oliver, Rep. Prog. Phys. **83**, 054401 (2020).

[23] C. Bauckhage, E. Brito, K. Cvejoski, C. Ojeda, J. Schücker, R. Sifa, In Proceedings of 14th Int. Workshop Mining and Learning with Graphs (MLG18). ACM, New York, NY, USA (2018).

[24] M. Sniedovich, Control and Cybernetics. **35**, 599 (2006)

[25] B. E. Husic, V. S. Pande, J. Am. Chem. Soc. **140** 2386 (2018)

[26] K. Müller and L. D. Brown, Theor. Chem. Acta (Berl.) **53**, 75 (1979).